

Biochemical Activities and Genetic Functions of the *Drosophila melanogaster* Fancm Helicase in DNA Repair

Noelle-Erin Romero,* Steven W. Matson,*[†] and Jeff Sekelsky*^{†,‡,1}

*Curriculum in Genetics and Molecular Biology, [†]Department of Biology, and [‡]Integrative Program for Biological and Genome Sciences, University of North Carolina, Chapel Hill, North Carolina 27599

ABSTRACT Repair of DNA damage is essential to the preservation of genomic stability. During repair of double-strand breaks, several helicases function to promote accurate repair and prevent the formation of crossovers through homologous recombination. Among these helicases is the Fanconi anemia group M (FANCM) protein. FANCM is important in the response to various types of DNA damage and has been suggested to prevent mitotic crossovers during double-strand break repair. The helicase activity of FANCM is believed to be important in these functions, but no helicase activity has been detected *in vitro*. We report here a genetic and biochemical study of *Drosophila melanogaster* Fancm. We show that purified Fancm is a 3' to 5' ATP-dependent helicase that can disassemble recombination intermediates, but only through limited lengths of duplex DNA. Using transgenic flies expressing full-length or truncated Fancm, each with either a wild-type or mutated helicase domain, we found that there are helicase-independent and C-terminal-independent functions in responding to DNA damage and in preventing mitotic crossovers.

KEYWORDS biochemistry; genetics; DNA helicase; homologous recombination; synthesis-dependent strand annealing; ATP activity; crossing over

DNA helicases are a diverse group of enzymes that separate the two strands of duplex DNA. Using the free energy derived from the hydrolysis of a 5' nucleoside triphosphate, generally ATP, the helicase catalyzes the unwinding of duplex DNA to yield single-stranded DNA (ssDNA), a process that is required in replication, transcription, recombination, and repair. Thus, helicases are involved in essentially all metabolic pathways that require the separation of duplex DNA (Brosh 2013; Khan *et al.* 2015).

Helicases exhibit a diversity of structure and mechanism that may be related to the often unique and specialized roles that these enzymes can play in the cell (Brosh 2013; Daley *et al.* 2013). Importantly, distinct helicases can interact with specific DNA substrates. For example, during repair of DNA damage, different helicases often act within particular pathways and on unique DNA intermediates that are generated as repair pro-

gresses, such as Holliday junctions (HJs) or displacement loops (D-loops). This can be observed in the requirement for helicases to recognize and act on specific DNA structures during the process of double-strand break (DSB) repair via homologous recombination (HR).

DSB repair by HR is a complex process with several key events: resection of the 5' end at the strand break; invasion of the Rad51-coated 3' ssDNA tail into a homologous duplex sequence, generating a D-loop; DNA synthesis primed from the invading 3' end; and resolution into one of either two types of recombination product—crossovers (COs) or noncrossovers (NCOs). The formation of COs during DSB repair in mitotically dividing cells can be hazardous as they can result in loss of heterozygosity and gross chromosomal rearrangements (Lorenz and Whitby 2006; Andersen and Sekelsky 2010). Therefore, prevention of CO pathways through the activation and promotion of NCO pathways is favored in mitotic cells undergoing HR to ensure genomic stability.

To prevent CO generation, helicases can act on several DNA intermediates generated during DSB repair via HR. During HR, an invading DNA strand from the homologous chromosome forms a D-loop as described above. After synthesis, the invading strand can be unwound from the template and annealed to the

Copyright © 2016 by the Genetics Society of America

doi: 10.1534/genetics.116.192534

Manuscript received June 10, 2016; accepted for publication July 18, 2016; published Early Online July 26, 2016.

Supplemental material is available online at www.genetics.org/lookup/suppl/doi:10.1534/genetics.116.192534/-/DC1.

¹Corresponding author: 303 Fordham Hall, Department of Biology, University of North Carolina, Chapel Hill, NC 27599-3280. E-mail: sekelsky@unc.edu

other resected end, resulting in an NCO; a process known as synthesis-dependent strand annealing (SDSA) (Adams *et al.* 2003). Alternatively, the displaced strand can anneal to the other resected end, leading to the formation of an entwined structure referred to as a double-Holliday junction (dHJ). The dHJ can be processed by structure-specific endonucleases, possibly giving rise to a CO, or acted upon by a helicase/topoisomerase complex in a process known as dissolution, generating a NCO (Daley *et al.* 2013). Thus, helicases are essential in the promotion of NCO products either through promotion of D-loop disassembly through SDSA or the dissolution of the dHJ, thereby preventing the formation of potentially deleterious COs during repair (Andersen and Sekelsky 2010; Heyer *et al.* 2010; Daley *et al.* 2013).

One family of conserved DNA helicases/translocases whose members are involved in HR regulation is related to archaeal helicase-associated endonuclease for fork-structured DNA (Hef) (Komori *et al.* 2002; Prakash *et al.* 2009; Zheng *et al.* 2011; Lorenz *et al.* 2012). *Pyrococcus furiosus* Hef contains a conserved DEAD-box helicase domain and an ERCC4 C-terminal endonuclease domain. Hef functions as a homodimer in cleaving DNA forks and processing HJs into splayed arms, indicating roles for this protein during DNA replication and repair (Komori *et al.* 2004). The domain structure of Hef is similar to that of the eukaryotic structure-specific endonucleases MUS81 and XPF, but they have inactive helicase domains (Nishino *et al.* 2005). Conversely, in Fanconi anemia group M (FANCM), the nuclease domain is inactive (Meetei *et al.* 2005; Ciccia *et al.* 2007; Ciccia *et al.* 2008).

Mutations in *FANCM* cause Fanconi anemia (FA), a hereditary disorder characterized by an increased incidence of cancer, developmental abnormalities, and bone marrow failure (Meetei *et al.* 2005). A classic hallmark of cells from FA patients is a heightened sensitivity to DNA interstrand cross-linking (ICL) agents, including the chemotherapeutic agents cisplatin and mitomycin C. The primary role of FANCM appears to be to target disrupted replication forks and promote CO avoidance by processing DNA intermediates that occur during DSB repair via HR (Prakash *et al.* 2005; Prakash *et al.* 2009; Nandi and Whitby 2012).

The *Saccharomyces cerevisiae* FANCM ortholog, Mph1, has also been shown to be involved in preventing COs (Prakash *et al.* 2009), and *mph1* mutants show sensitivity to DNA-damaging agents such as ionizing radiation (IR) and methyl methanesulfonate (MMS) (Scheller *et al.* 2000). Biochemical studies using purified Mph1 show that it is a 3' to 5' DNA helicase capable of unwinding Rad51-coated D-loops (Prakash *et al.* 2005; Prakash *et al.* 2009), and that it can process DNA intermediates that form later in repair, including HJs (Prakash *et al.* 2005; Prakash *et al.* 2009; Kang *et al.* 2012). Unwinding of HJs and D-loops has also been observed using the *S. pombe* ortholog Fml1 (Sun *et al.* 2008). In contrast, no helicase unwinding activity has been detected for human FANCM (Meetei *et al.* 2005; Gari *et al.* 2008). Together, genetic and biochemical studies suggest roles for FANCM and its orthologs in HR that are dependent upon their ability to use ATP hydrolysis to unwind or

remodel DNA structures so as to prevent COs (Prakash *et al.* 2009; Lorenz *et al.* 2012; Mazón and Symington 2013; Mitchel *et al.* 2013; Kuo *et al.* 2014).

FANCM and orthologs may also have roles that are not dependent on catalytic activity. The C-terminal of human FANCM, like its Hef ancestor, has an ERCC4-like endonuclease domain. Although this domain is considered to be catalytically dead, it is involved in protein-protein interactions (Huang *et al.* 2010; Wang *et al.* 2013; Yang *et al.* 2013). Yeast and human FANCM have several motifs in the C-terminal that facilitates interaction with chromatin, additional FA proteins, and repair complexes (Deans and West 2009; Vinciguerra and D'andrea 2009). In human FANCM, two specific motifs (MM1 and MM2) have been shown to allow for interaction with the FA complex and the Bloom syndrome helicase (BLM) complex, which is involved in DSB repair via HR (Deans and West 2009). While these two motifs are not detected in yeast and *Drosophila* orthologs, there is still the potential for C-terminal interactions with other proteins involved in HR or DNA repair complexes.

A previous genetic study in our laboratory has shown that *Drosophila* Fancm, like its orthologs, is involved in the prevention of COs (Kuo *et al.* 2014). This study tested the response of Fancm in CO prevention and response to DNA-damaging agents. To better understand the role of the Fancm helicase activity in directing homologous recombination toward a NCO product, we tested the ability of the purified Fancm helicase to act on HR repair intermediates *in vitro*. We generated Fancm ATP hydrolysis mutants *in vivo* to examine the role of the helicase in responding to DNA damage and CO prevention. We also sought to understand the role, if any, of the C-terminal of Fancm in regulating repair events in *Drosophila*. We generated C-terminal truncations of Fancm *in vivo* and analyzed how these mutants respond to various DNA-damaging agents and their function in CO prevention.

Here we show that purified Fancm can unwind duplex DNA in a 3' to 5' direction in an ATP-dependent manner. Further, we provide evidence that Fancm can disassemble the HR D-loop intermediate. *In vivo* work used to study the role of the helicase activity and the C-terminal domain of Fancm reveals that Fancm lacking either helicase activity or the C-terminal is able to prevent some mitotic COs and respond to DNA damage.

Materials and Methods

Expression and purification of *Drosophila* FANCM

Truncated FANCM, lacking 840 C-terminal residues (Fancm Δ), was cloned into pLIC-His- maltose binding protein (MBP) using InFusion cloning (Clontech), with primers FAM1 and FAM2 (Supplemental Material, Table S1) and complementary DNA (*Drosophila* Genomics Resource Center). The K84M (Fancm Δ ^{KM}) mutation was introduced into Fancm Δ using the QuickChange Site-Directed Mutagenesis Kit (Agilent Technologies) with the pLIC-HisMBP-Fancm Δ construct as the template and the KMQC primer (Table S1). The protein expression plasmid was maintained in *Escherichia coli* BL21DE3/pLysS

and protein expression was induced by auto-induction (Studier 2005, 2014). Bacterial cultures were grown in 3 liters of ZYM5052 auto-induction medium (Studier 2005) at 25° for 24 hr. Cells were harvested by centrifugation, washed with 20 ml of sodium chloride-Tris-EDTA buffer (10 mM Tris-HCl, pH 8.0, 1 mM EDTA, and 100 mM NaCl), harvested again by centrifugation and stored as a cell pellet at -80° until use.

Drosophila Fancm Δ and Fancm Δ^{KM} were purified to near homogeneity (Figure S1) using Ni-NTA Resin (QIAGEN, Valencia, CA) and Amylose Resin (New England Biolabs, Beverly, MA) to take advantage of the two affinity tags present on the fusion protein. Cells were lysed in Buffer L (500 mM NaCl, 50 mM Tris-HCl, pH 7.0, 10% glycerol) with 100 mM PMSF, EDTA-free protease inhibitor cocktail, 0.1% triton X-100 and 1 mg/ml lysozyme by incubation at 4° for 45 min and then sonicated to reduce viscosity in 10-sec bursts. Cleared lysate, isolated by centrifugation, was incubated with 3-ml Ni-NTA resin, and 12-column volumes of Buffer L were flowed through the column. Protein was eluted using 300 mM imidazole in Buffer L and protein was detected using a Bradford assay (Bio-Rad, Hercules, CA). Peak fractions were concentrated and the buffer was exchanged with Buffer M (200 mM NaCl, 20 mM Tris-HCl, pH 7.4, 1 mM EDTA) using Amicon Ultra, Ultracel 50K Centrifugal Filters (Millipore, Bedford, MA). The protein was then bound to a 1.5-ml Amylose column, washed with 10-column volumes of Buffer M, and the protein was eluted in Buffer M with 50 mM maltose and 10 mM dextrose. Protein was detected by Bradford assay and dialyzed against storage buffer (150 mM NaCl, 50 mM Tris-HCl, pH 7.0, 10% glycerol, 0.1 mM EDTA) and stored at -20°. Protein purity was evaluated using SDS-PAGE.

DNA substrates

Synthetic oligonucleotides (Table S1) used for DNA substrate preparation were PAGE purified by the supplier (Integrated DNA Technologies). Radioactively labeled substrates were prepared by incubating 10 pmol oligonucleotide with 3 μ M [γ -³²P]ATP and T4 polynucleotide kinase (New England Biolabs) at 37° for 50 min, followed by a 20 min incubation at 70° to inactivate the enzyme. Labeled oligonucleotide was then annealed to its complement oligonucleotide in a ratio of 1:1.3 labeled:unlabeled oligonucleotide for fork substrates, or 1:1.3:1.3 labeled:unlabeled oligonucleotide for D-loop substrates. Annealing occurred in Buffer A (50 mM NaCl, 10 mM Tris-HCl, pH 7.5, 1 mM MgCl₂) by heating at 95° for 5 min and slowly cooling to room temperature. Hybridized DNA substrates were separated from unannealed oligonucleotide and free [γ -³²P]ATP using a Sephadex G-50 column (Pharmacia LKB, Piscataway, NJ).

ATPase assays

ATPase reactions were conducted using 212 nM of either Fancm Δ or Fancm Δ^{KM} . Reaction mixtures (20 μ l) contained Buffer C (25 mM Tris-HCl, pH 7.5, 20 mM NaCl, 5 mM 2-mercaptoethanol, 10 μ g/ml BSA), M13mp18 ssDNA titrated from 0 to 120 nM (nucleotide phosphate), and 3 mM MgCl₂.

For ATPase reactions that used dsDNA, pET15b plasmid that was cut with the restriction enzyme *Hpa*I, extracted using phenol:chloroform, and precipitated with NaOAc, was used. All reagents except ATP were mixed and allowed to incubate on ice. ATP with a concentration of 3 mM and with trace amounts (~60 nCi/ μ l) of [γ -³²P]ATP was added to initiate the reaction, and incubation was at 37° for 5 min. Aliquots (5 μ l) were removed, and stop solution (5 μ l) was added to a final concentration of 17 mM EDTA, 3.4 mM ATP, and 3.4 mM ADP. Of this mixture, 2 μ l was spotted onto a cellulose matrix TLC- polyethylene terephthalate plate (Sigma Chemical, St. Louis, MO) and developed in a 0.8 M LiCl/1 M formic acid solution. Plates were allowed to dry, exposed on a phosphor storage screen, and imaged using a Phosphorimager (Amersham, Piscataway, NJ). All images were quantified using ImageQuant software.

Helicase assays

Steady-state helicase unwinding reaction mixtures (20 μ l) contained 0.1 nM radiolabeled DNA substrate (Table S1), 25 mM Tris-HCl (pH 7.5), 3 mM MgCl₂, 20 mM NaCl, 5 mM 2-mercaptoethanol (β ME) and 10 μ g/ml BSA. Protein was titrated from a concentration of 0.5 to 212 nM. Reactions were initiated by the addition of 3 mM ATP, incubated at 37° for 15 min and stopped with the addition of 10 μ l of helicase stop solution (37.5% glycerol, 50 mM EDTA, 0.3% SDS, 0.5 \times TBE, 0.1% bromophenol blue). All reactions were resolved on 7.5% nondenaturing polyacrylamide gels containing 0.5 \times TBE and 0.1% SDS, at room temperature for 2 hr at 180 V. Gels were transferred to Whatman paper, allowed to soak for 30 min in drying buffer (40% methanol, 10% acetic acid, 3% glycerol), and dried for 6 hr using a gel dryer. Dried gels were exposed on a phosphor storage screen and imaged using a Phosphorimager (Amersham). All images were quantified using ImageQuant software.

Fluorescence anisotropy

Reaction mixtures (50 μ l) contained 10 nM 5' fluorescently labeled 6-carboxyfluorescein DNA substrate (Table S1), 25 mM Tris-HCl (pH 7.5), 3 mM MgCl₂, 20 mM NaCl, 5 mM β ME, and 10 μ g/ml BSA. Fluorescence anisotropy was measured as a function of Fancm concentration from 1 to 212 nM. Reactions were incubated at 25° for 5 min. Fluorescence anisotropy was measured using a Jobin Yvon Horiba Fluorolog-3 fluorometer with a Wavelength Electronics temperature-control box. Labeled dsDNA substrates were excited at 495 nm and emission was measured at 520 nm. Fluorescence anisotropy was calculated using the software provided by the instrument.

Drosophila stocks

Fly stocks were maintained at 25° with standard medium. *Fancm*⁰⁶⁹³ is a nonsense mutation previously described in Kuo *et al.* (2014). Deletion of endogenous *Fancm* (*Fancm*^{del}) was generated using clustered regularly interspaced short palindromic repeats (CRISPR)/Cas9 technology (Bassett *et al.* 2013; Gratz *et al.* 2013). Oligonucleotides (Integrated DNA

Technologies) used for guide RNA (Del1 and Del2; Table S1) were cloned into pU6 Bbs1 chimeric RNA vector, and this was injected into Cas9(X) (BestGene). *Fancm^{del}* deletes 3R: 21480913 to 3R: 21487017. In experiments reported here, *Fancm* mutants were *st Fancm⁰⁶⁹³/Sb Fancm^{del}*, or *st Fancm⁰⁶⁹³/w+transgene Sb Fancm^{del}*, expressed under the endogenous *Fancm* promoter. Plasmids used for injections of transformants were generated from a PCR-amplified genomic fragment (F1 and F2, Table S1). The K84M mutation was introduced using the QuickChange Site-Directed Mutagenesis Kit (Agilent Technologies) and Primer KMQC (Table S1). The truncated *Fancm¹⁻⁶⁴⁵* construct was generated from the full-length (FL) construct using endogenous *MfeI* sites. Infusion reaction was used to add the C-terminal and 3' UTR with a PCR reaction and primer FA (Table S1) from the original construct. *Fancm^{1-645K84M}* was generated in the same way, using the FL Walker A mutant (FLKM) construct. RT-PCR (QIAGEN) was used to determine expression (Figure S1) using primers RT (Table S1).

Mitotic CO assay

Mitotic COs were measured in the male germline as previously described (McVey *et al.* 2007), using the genetic markers *st* and *Sb* for each genotype indicated. At least 20 individual males were assayed for each genotype indicated. Statistical analyses and graphing were done in Prism 6 (GraphPad) using the Kruskal–Wallace test. *P*-values reported are corrected for multiple comparisons.

DNA damage sensitivity assays

Sensitivity to DNA-damaging agents was determined as previously described (Yildiz *et al.* 2004). Briefly, an aqueous solution of either MMS or mechlorethamine (HN2) at the indicated concentrations was added to the food during larval feeding. Adults in untreated vials were allowed to mate and lay eggs for 3 days before being transferred into fresh vials, allowed to lay eggs for 2 days, and treated with DNA-damaging agents. For IR, larvae were exposed to gamma rays in an irradiator at 1500 rad. At least 10 biological replications were performed for each genotype indicated. Relative survival was calculated for each vial as the ratio between mutant to control flies in treated vials and normalized to the ratio of mutant to control flies in the untreated vial. Vials with <20 progeny were discarded. Statistical analyses were performed as described above.

Data availability

The authors state that all data necessary for confirming the conclusions presented in the article are represented fully within the article.

Results and Discussion

Fancm is an ssDNA-dependent ATPase

Previous genetic studies of *Drosophila Fancm* indicated a role for the protein in SDSA and in preventing mitotic COs (Kuo *et al.* 2014). To further understand roles of *Fancm* in DNA

repair, we investigated the biochemical properties of purified *Fancm*. Superfamily 2 helicases, including *Fancm*, are characterized by several conserved motifs, including a Walker A motif that binds the triphosphate tail of ATP and consequently plays a role in ATP hydrolysis (Walker *et al.* 1982; Koonin 1993). We were unable to express and purify FL *Fancm*, so a truncated form of *Fancm* (*Fancm* Δ) and a truncated form with a mutation in the Walker A motif (*Fancm* Δ ^{KM}) were overexpressed as His6x-MBP tagged proteins (Figure 1A) in *E. coli*, and each was purified to near homogeneity (Figure S2). This truncation was generated to encompass the entire helicase domain and is based off of purified truncations of the fission yeast ortholog, *Fml1* (Sun *et al.* 2008).

We confirmed the ATPase activity of purified *Fancm* Δ and measured several biochemical parameters to characterize this activity (Figure S3). There was no detectable ATP hydrolysis in the absence of DNA, whereas the ATPase activity of the purified protein was higher in the presence of circular M13 ssDNA compared to that of dsDNA, confirming that the protein is a DNA-dependent ATPase (Figure 1B). In addition, we measured the effective rate constant (K_{eff}) and the V_{max} for ssDNA (K_{eff} , 2.8 μM ; V_{max} , 65.3 pmol) and dsDNA (K_{eff} , 5.7 μM ; V_{max} , 40.1 pmol), under these conditions, further confirming that ssDNA stimulates ATPase activity more strongly than dsDNA. As expected, the *Fancm* Δ ^{KM} mutant lacked ATPase activity (Figure 1B). Taken together, these results indicate that *Fancm* is a DNA-dependent ATPase and this activity is dependent on the lysine residue found in the canonical helicase motif I (Figure 1A). ATPase activity stimulated by ssDNA as well as dsDNA has been reported for human FANCM and yeast *Fml1*, while *Mph1* only exhibits ssDNA-dependent activity (Meetei *et al.* 2005; Prakash *et al.* 2005; Nandi and Whitby 2012). Fluorescence anisotropy was used to determine if differences in ATPase stimulation were a result of DNA binding (Figure S4). No significant differences in binding to ssDNA vs. dsDNA were detected for the truncated protein.

Fancm is a 3' to 5' DNA helicase

To determine if *Drosophila Fancm* is active as a helicase, unwinding assays were performed using partial duplex substrates under steady-state conditions. Purified protein was incubated with DNA substrate and the reaction was initiated by the addition of ATP. The wild-type (*Fancm* Δ) helicase completely unwound a 15-bp partial duplex substrate with a 25-bp 3' ssDNA tail (15/40) (Figure 1C, third lane). There was no detectable unwinding of the substrate at an equal concentration of mutant protein *Fancm* Δ ^{KM} (Figure 1C, fourth lane). When the same reaction was conducted with a 15-bp partial duplex with 25-bp 5' ssDNA tail (–15/40), the wild-type helicase failed to unwind the substrate (Figure 1D). Fluorescence anisotropy was used to determine if there was a difference in binding of *Fancm* Δ to these structures. No significant difference in binding affinity was detected when *Fancm* was incubated with partial duplex structures with either a 3' or 5' ssDNA tail (Figure S4); indicating that unwinding of the protein is a result of a directional bias and classifies *Fancm* as a 3' to 5' helicase, consistent

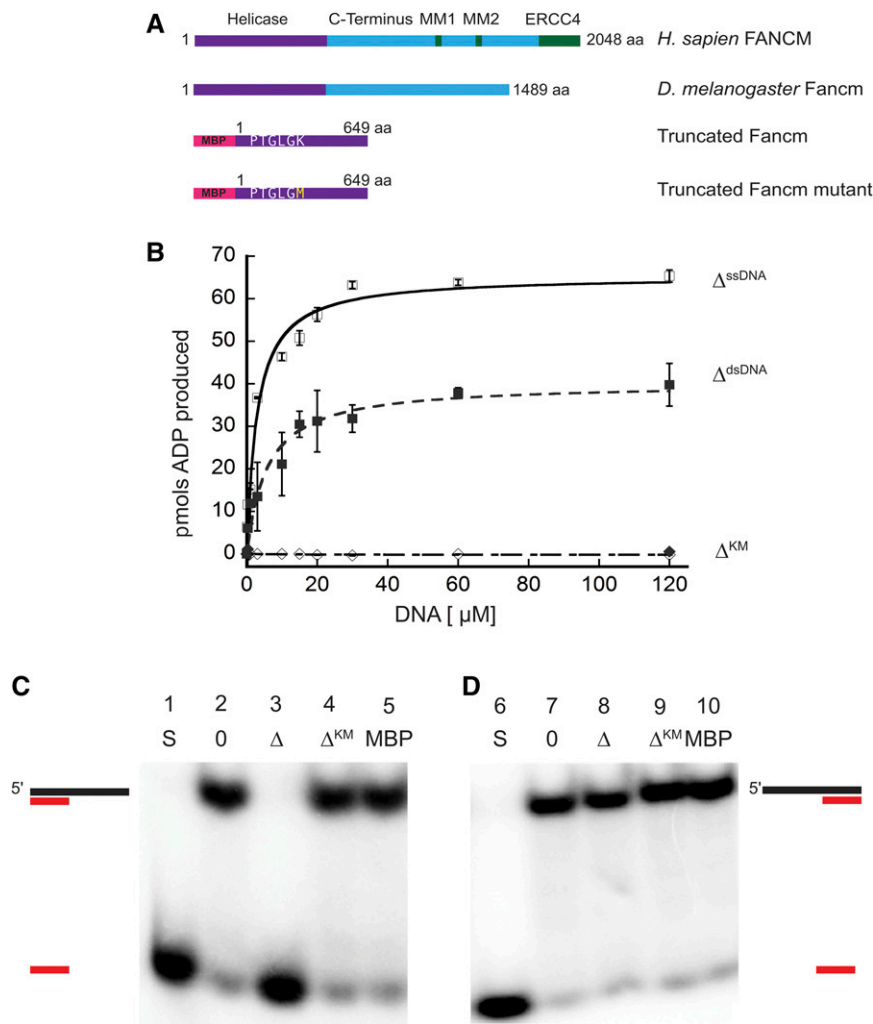


Figure 1 *Drosophila* Fancm is a 3' to 5' DNA helicase dependent on ATP hydrolysis. (A) Schematic of Fancm. Domains and motifs present in human FANCM are marked. Conserved domains or motifs in *D. melanogaster* are noted. Truncated forms depicted are with an N-terminal MBP tag. (B) ATP hydrolysis by Fancm. Fancm ATPase activity was examined as a function of DNA concentration using either M13mp18 ssDNA (\square) or dsDNA (\blacksquare) as the DNA cofactor. All reactions were incubated at 37° for 5 min. \square \blacksquare 212 nM Fancm Δ on ssDNA (Δ^{ssDNA}); \diamond \blacklozenge 212 nM Fancm Δ^{KM} (Δ^{KM}). The average values from at least three independent experiments were plotted. Error bars represent SEM (ssDNA) or SD of the mean (dsDNA). (C) Fancm unwinds duplex DNA. Protein (212 nM) was incubated with a 5' radiolabeled 15-bp partial duplex with a 25-nt 3' overhang (15/40). (D) Fancm is a 3' to 5' DNA helicase. Protein (212 nM) was incubated with a 5' radiolabeled 15-bp partial duplex with a 25-nt 5' overhang (–15/40). Lane 1 and 6 (S) are boiled loading controls indicating ssDNA. Lanes 2 and 7 (0) are no-protein controls. Fancm Δ in lane 3 and 8 (Δ), Fancm Δ^{KM} in lane 4 and 9 (Δ^{KM}), and MBP in lane 5 and 10 (MBP). Colored strand represents radiolabeled strand. Substrate oligonucleotides are in Table S1.

with previous work on orthologs (Prakash *et al.* 2005). These data also support the conclusion that Fancm cannot unwind blunt-ended duplex DNA, as no unwinding of the –15/40 substrate was detected even at longer incubation times.

As shown in Figure S5, no unwinding of the 15/40 substrate was detected when either ATP or MgCl₂ were omitted from the reaction. Moreover, unwinding was undetectable when the nonhydrolyzable ATP analog AMP-PNP was substituted for ATP. Taken together, these data indicate that unwinding by the Fancm helicase is dependent upon the ability of the protein to hydrolyze ATP and the Fancm Δ^{KM} mutant is a “helicase-dead” protein.

Fancm has limited unwinding capability

Further testing of the helicase activity of Fancm revealed a limit in unwinding longer regions of duplex DNA. A substantial decrease in unwinding activity was observed using a 20-bp partial-duplex substrate with a 20-bp 3' ssDNA tail (20/40). Only 60% of the DNA substrate was unwound by the wild-type helicase at a concentration of protein that unwound all of the 15/40 partial duplex substrate (Figure 2A). To exclude the possibility that the reduced length of the free 3' tail was responsible for this result,

we generated a 20-bp partial-duplex substrate with a 25-bp 3' ssDNA tail (20/45). As seen with the 20/40 substrate, Fancm was only able to unwind 60% of the 20/45 substrate (Figure 2A). We also measured unwinding activity using two splayed-arm substrates, one with a 3' single-stranded region of 25 bp, and one with a 3' single-stranded region of 20 bp; both substrates had a 15-bp duplex region. Both substrates were completely unwound, indicating that neither the length of the 3' tail nor the complexity of the substrate affects unwinding (Figure S6A). An additional splayed-arm substrate with a 25-bp duplex region and 25-nt 5' and 3' ssDNA arms was also tested (Figure 2A), with no detectable unwinding.

To test if the initial rate of the reaction or the duration of the reaction affected unwinding, unwinding for each substrate was determined using 10 and 150 nM protein at various time points for the 15/40 and 20/40 substrates used (Figure 3, A and B). At 10 nM protein concentration (Figure 3A), Fancm Δ was able to fully unwind the 15/40 substrate over the course of the experiment, but could unwind only 37% of the 20/40 substrate. The same is true for reactions using 150 nM protein (Figure 3B). These data indicate that the inability to unwind the 20/40 substrate, even after extended incubation, is not due to the

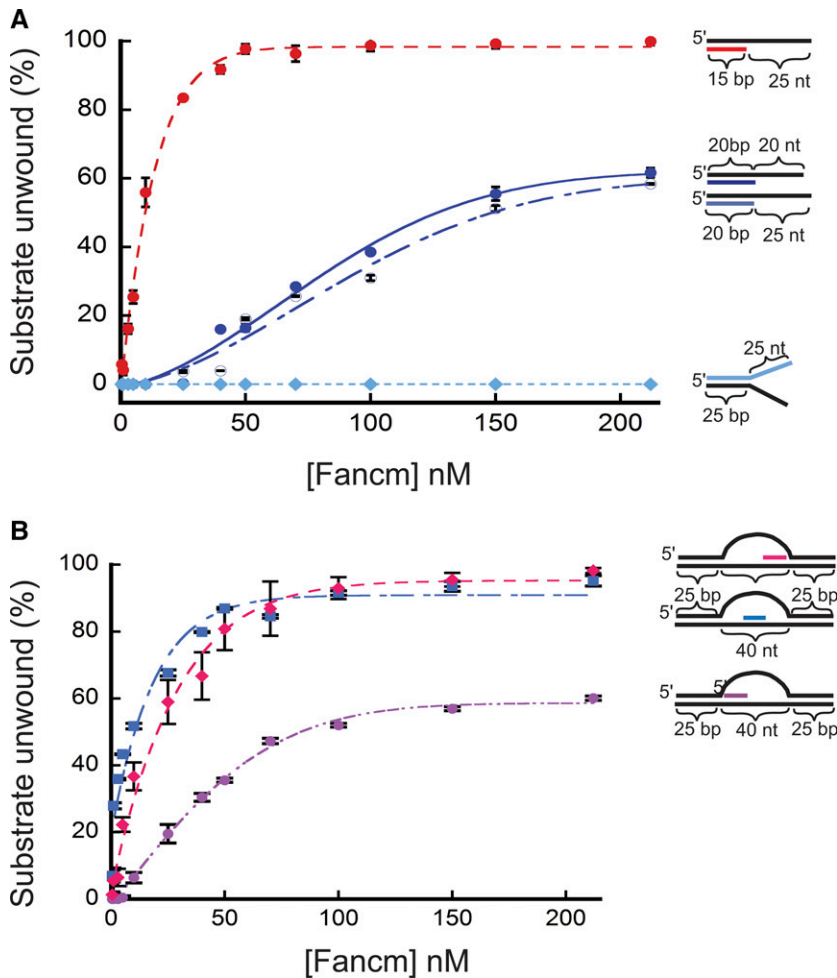


Figure 2 Unwinding of partial duplex DNA substrates by Fancm. Helicase reactions were performed as described in *Materials and Methods*. The indicated concentrations of Fancm were incubated with 0.1 nM of the indicated substrate for 15 min. Colored strand on each substrate represents radiolabeled 5' strand. Quantitative data from at least three experiments were plotted as the average for each protein concentration. Error bars represent the SEM. Oligonucleotides used to make these substrates can be found in Table S1. (A) Comparison of the fraction of substrate unwound with partial duplex substrates of different duplex lengths. Pink ●, 15-bp duplex region with a 25-nt overhang. Blue ●, 20-bp duplex region with a 20-nt overhang. Blue ○, 20-bp duplex region with a 25-nt overhang; Blue ◆, 25-bp duplex region with 25-nt single-stranded arms. (B) Unwinding of D-loop intermediate substrates by Fancm. Pink ●, front; blue ■, middle; pink ◆, end. Bubble structures were made using a two 90-nt oligonucleotides with 25 bp of complementary ends with a 40-nt noncomplementary middle (A1/A2). Substrate oligonucleotides are in Table S1.

presence of inactive protein in the preparation or to loss of activity during the course of the reaction.

The inability of Fancm to catalyze unwinding of greater lengths of duplex DNA may result from the use of a truncated protein or missing factors such as post-translational modifications or interacting proteins. Alternatively, the limited helicase may be an intrinsic property of this protein. Similar truncation of Fml1 did not appear to limit the length of duplex unwinding (Nandi and Whitby 2012). Conversely, there are cases where inclusion of sequences predicted to be unstructured, like the C-terminal of Fancm, impedes activity *in vitro*. An example is Blm helicase, where the FL protein cannot unwind nucleosomal DNA but a protein that has only the conserved helicase domain can (Fujimoto *et al.* 2009). Thus, while we cannot exclude the possibility that *Drosophila* Fancm unwinds longer duplex regions *in vivo*, we hypothesize that the limited unwinding ability we observed is reflective of the protein's functions in DNA repair.

Based on *in vivo* data (Kuo *et al.* 2014), we hypothesized that Fancm may be involved in SDSA by displacing D-loops. In previous yeast studies it was shown that Mph1 can unwind the D-loop structures generated during recombination (Prakash *et al.* 2009). To test the ability of Fancm to unwind complex structures, we constructed substrates resembling a recombination D-loop intermediate. We incubated Fancm with a 40-nt

bubble-like structure containing an “invading” homologous strand in which the duplex region was limited to 15 bp. To determine whether position of the invading strand had an effect on unwinding, the invading strand was positioned at the “front”, “middle”, and “end” of the homologous template strand within the bubble (Figure 2B). Fancm catalyzed robust unwinding of substrates with the invading strand positioned in the middle and at the end of the bubble. However, Fancm unwound the substrate with the invading strand positioned at the front with much lower efficiency. The decrease in substrate unwound as the position of the duplex region is moved is most likely not a result of the length of the duplex region, but rather of the ability of Fancm to access the duplex region. This is possibly a result of a lack of an ssDNA region to which the helicase can bind to initiate unwinding. The middle and end both have regions that mimic the partial duplex with an ssDNA 3' tail. However, the front position substrate does not have a partial duplex with an ssDNA 3' tail, but instead has a 5' ssDNA tail. As shown above, Fancm does not catalyze unwinding of a substrate with a 5' ssDNA tail (see Figure 1D). However, in this more complex substrate, there is an open ssDNA region on the opposite strand of the bubble. Fancm most likely unwinds enough of the duplex arm, generating a 3' tail, and thereby catalyzing unwinding of the invading strand. When a 5' ssDNA tail was added to more

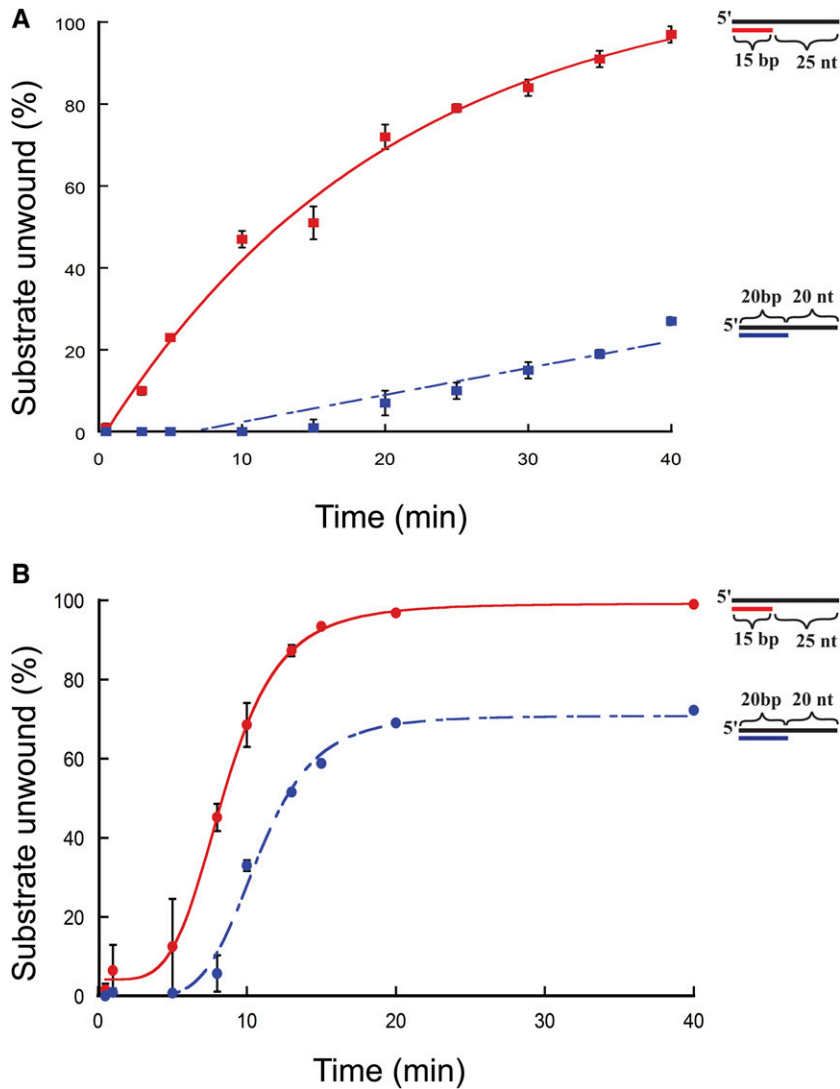


Figure 3 Time-course unwinding of partial-duplex DNA substrates by Fancm. Helicase reactions were performed as described in *Materials and Methods*. The indicated concentrations of Fancm were incubated with 0.1 nM of the indicated substrate for the indicated time. Colored strand on each substrate represents radiolabeled 5' strand. Quantitative data from at least three experiments were plotted as the average for each protein concentration. Error bars represent the SEM. Oligonucleotides used to make these substrates can be found in Table S1. (A and B) Comparison of the fraction of substrate unwound with 10-nm Fancm Δ on partial-duplex substrates at the indicated time points of different duplex lengths. (A) Red \blacksquare , 15-bp duplex region with a 25-nt overhang (15/40); blue \blacksquare , 20-bp duplex region with a 20-nt overhang (20/40). (B) Red \bullet , 15-bp duplex region with a 25-nt overhang (15/40); blue \bullet , 20-bp duplex region with a 20-nt overhang (20/40). Substrate oligonucleotides are in Table S1.

closely mimic an invading strand, no difference in unwinding was detected (Figure S6B).

The data presented here indicate that Fancm as a 3' to 5' DNA helicase that is able to unwind up to 20 bp of partial-duplex DNA substrates in an ATP-dependent manner. In addition, the enzyme is able to dissociate short duplex regions in more complex D-loop-like structures. The failure of the protein to unwind longer duplex regions may be the result of *in vitro* conditions or lack of an important accessory protein or modification. Efforts to detect unwinding of longer duplex regions in the presence of an ssDNA binding protein (*E. coli* SSB) or under other conditions (e.g., different salt concentration) were unsuccessful.

Mph1 and Fml1 have both been shown to be active helicases unwinding up to 100 bp of duplex DNA (Prakash *et al.* 2005). On the other hand, human FANCM has been shown to migrate D-loops and HJs, but no unwinding activity has been reported (Meetei *et al.* 2005; Prakash *et al.* 2005; Gari *et al.* 2008; Sun *et al.* 2008; Zheng *et al.* 2011). The data presented here suggest that *Drosophila* Fancm, while similar to both the yeast and human orthologs, is unique. Unlike human FANCM, it is an

active helicase, yet we could not detect unwinding of longer duplex regions like Mph1 and Fml1. Although we were not able to detect DNA unwinding by the protein of duplex regions of >20 bp, there may be other factors that can contribute to an increase in helicase activity. The unwinding activity of Mph1 is stimulated by the addition of replication protein A (RPA) (Prakash *et al.* 2005); although SSB did not stimulate unwinding activity of Fancm, it is possible that *Drosophila* RPA or other proteins would do so.

Helicase-dead and truncated Fancm are each able to prevent a subset of mitotic COs

The C-terminal region of Fancm in yeast and human orthologs contains motifs that facilitate protein-protein interactions. Human FANCM has a helix-hairpin-helix region in its ERCC4-like domain that allows for association with FAAP24, an interaction that helps stabilize the protein on chromatin (Huang *et al.* 2010; Wang *et al.* 2013). The presence of human FANCM motifs 1 and 2 (MM1 and MM2) allow the interaction of FANCM with the FA core complex and the BLM complex, respectively (Deans

and West 2009; Hoadley *et al.* 2012). It should be noted that *Drosophila* *Fancm* has neither the ERCC4 domain nor recognizable MM1 or MM2 motifs. The lack of these sequences is consistent with the fact that the interacting partners associated with these domains, FAAP24, FANCA, and RMI1, are not present in *Drosophila* (FAAP24 appears to be missing from all insects, FANCA from holometabolous insects, and RMI1 from Schizophoran flies; unpublished observations). Nonetheless, it is likely that the C-terminal region of *Fancm*, although lacking any recognizable motifs found in orthologs, may contribute to the regulation and function of the protein.

To identify the role the C-terminal has in regards to function of the protein in regulation of HR, we generated transgenic recombinant flies expressing either FL or truncated *Fancm*. The truncated transgenic recombinant flies are identical to the *Fancm* Δ protein characterized *in vitro*, except that it lacks the His and MBP tags. We refer to the transgenic truncated *Fancm* as *tr* to distinguish it from *Fancm* Δ that has these tags. To investigate the role of the helicase activity in CO prevention and DNA-damage response, we generated transgenic recombinant flies that express either FL or truncated *Fancm* with either a wild-type helicase domain or the helicase-dead mutation used *in vitro* (Figure 1A and Figure 3A).

Previous reports on functions of *Drosophila* *Fancm* used the nonsense mutation *Fancm*⁰⁶⁹³ (L78ter) in *trans* to *Df(3R)ED6058*, a 423.1-kb genomic deletion that removes >50 genes (Kuo *et al.* 2014). To ensure that any mutant phenotype described was an effect of loss of *Fancm* and not the heterozygous deletion of surrounding genes, we used CRISPR technology to generate a partial deletion of *Fancm* (*Fancm*^{del}) that should result in no protein being produced. The mutants used here were heteroallelic for *Fancm*^{del} and *Fancm*⁰⁶⁹³. *Fancm* transcript is undetectable in the null background, indicating that no endogenous *Fancm* is being produced in flies of this genotype (Figure S1). In all assays performed, no significant difference was observed between the previous results using *Df(3R)ED6058* and our experiments using *Fancm*^{del}, allowing us to conclude that *Fancm*^{del} is a null allele and the previous experiments with the deficiency can be attributed to loss of *Fancm*. All subsequent experiments reported here used one copy of the transgene in the *Fancm*^{del}/*Fancm*⁰⁶⁹³ null background, and comparisons are made in reference to the null genotype.

As previously reported, *Fancm* mutants exhibit a significant increase in the number of spontaneous mitotic COs (Kuo *et al.* 2014). We assayed spontaneous mitotic COs in the male germline since meiotic COs do not occur in males. COs were scored between the visible markers *st* and *Sb* (~20% of the genome) (Figure 4A). No COs were detected in wild-type males or in *Fancm* null mutants with the FL transgene (Figure 4C), indicating that the transgenes used are fully functional and that *Fancm* is indeed involved in preventing mitotic COs. Flies with the truncated Walker A mutant (*trKM*) transgene showed an increase in COs similar to that of the null mutants. The presence of an active *Fancm* helicase domain without the C-terminal (*tr*) reduced the rate of spontaneous mitotic COs to near wild-type levels. Interestingly, the FLKM also reduced CO levels (Figure

4C). The fact that *tr* and FLKM reduced CO levels to near wild type yet *trKM* did not, indicates that there are at least two partially independent functions of *Fancm* in preventing COs: one that requires the helicase activity but not the C-terminal, and another that is dependent on the C-terminal but does not require helicase activity.

Although both FLKM and the *tr* transgenes reduced the levels of spontaneous mitotic COs seen in the null mutant, COs were still detected above wild-type levels. The difference between these genotypes and wild type does not cross the threshold typically used to be considered statistically significant, but we have never detected a CO in any wild-type male (McVey *et al.* 2007; Kuo *et al.* 2014; Lafave *et al.* 2014); hence, we believe the elevation is biologically significant. These data indicate that *Fancm* must be both FL and catalytically active to prevent all mitotic COs. However, the presence of either the FL helicase-dead protein, or the absence of the C-terminal but with retention of ATPase activity, is sufficient to prevent most mitotic COs.

Separation of function in *Fancm*'s roles in the response to DNA damage

Since the mitotic CO assay measures spontaneous germline COs detected in progeny, we cannot determine how or when COs are occurring. We therefore cannot provide a mechanistic explanation for the difference between the COs seen in FLKM and the COs in *tr*. The difference in CO phenotype found among the transgenes of *Fancm* led us to investigate whether there was a difference in DNA damage response using the transgenes described above.

Previous sensitivity studies using *Drosophila* *Fancm* showed that *Fancm* mutants were sensitive to the cross-linking agent HN2, the alkylating agent MMS, and strand breakage induced by IR (Kuo *et al.* 2014). These types of damage engender a variety of DNA-repair mechanisms. Since HN2 can induce mono-adducts, intrastrand cross-links, and ICLs, the alkylating agent MMS was tested to distinguish between the role of *Fancm* in repair of ICLs vs. a broader role in damage repair. While both MMS and HN2 damage can involve replication fork impairment, the cross-links induced by HN2 could lead to DSBs (Muniandy *et al.* 2010; Clauson *et al.* 2013). IR was therefore used to determine if *Fancm* is involved in repair of DSBs.

As previously reported, *Fancm* null mutants were sensitive to all damaging agents tested. The sensitivities seen in the null mutants are rescued when the FL transgene is present (Figure 4, B and D–F). The FL mutant (FLKM) and *tr* transgene both rescued sensitivity to HN2 and IR, but not MMS (Figure 4, B and D–F). The *trKM* transgene failed to rescue sensitivity to HN2 and IR, but did appear to rescue MMS sensitivity (Figure 4, B and D–F). However, progeny with the *trKM* transgene have delayed developmental timing. If MMS is unstable after addition to the culture medium, it is possible that control larvae ingested food immediately after addition of MMS, whereas *trKM* larvae ingested food at a later time, after a substantial fraction of MMS was already degraded. Because of this complication, we cannot be confident that the higher relative survival

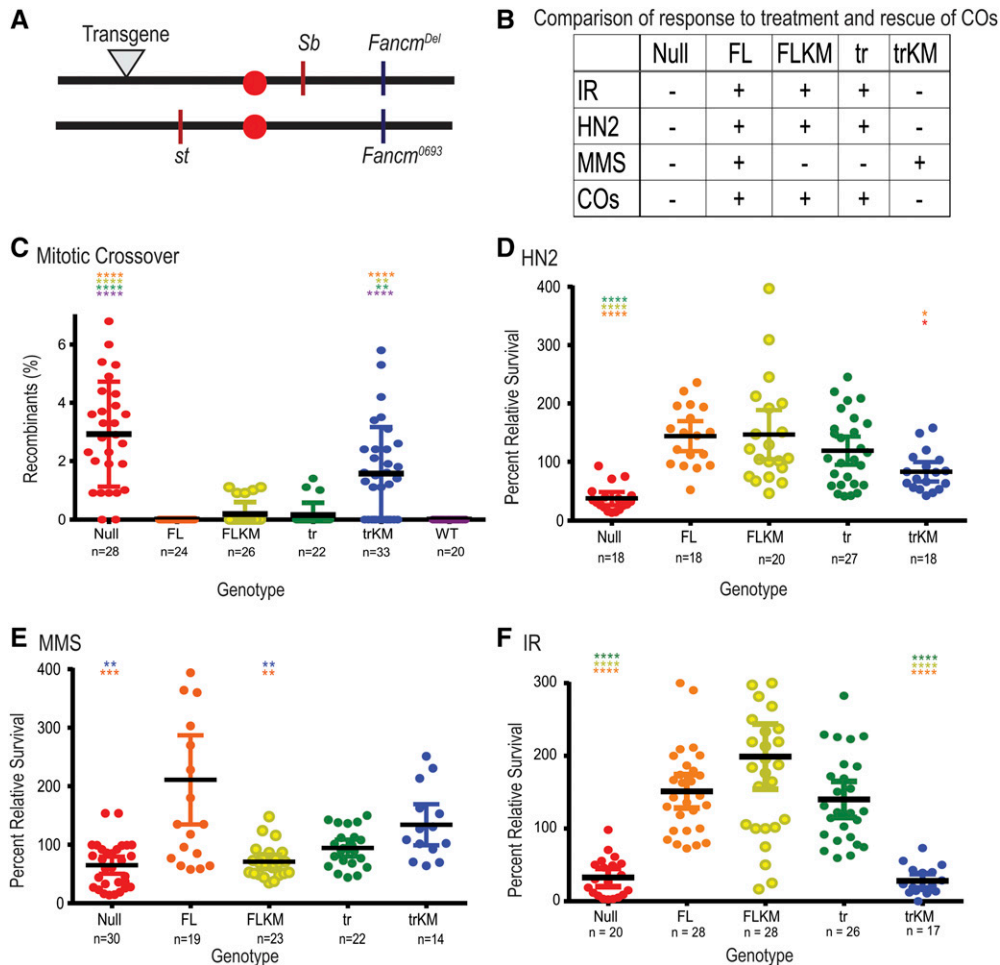


Figure 4 *Fancm* has genetically separable functions. (A) Map of *Fancm* null allele (*Fancm*⁰⁶⁹³), CRISPR deletion (*Fancm*^{Del}), transgene landing site (▽), and *st* and *Sb* genes. Schematic of transgenes generated are as seen in Figure 1A, without tags. (B) Table comparison of all transgenic *Fancm* genotypes and null genotype. – indicates no rescue of the null phenotype, + indicates rescue. (C) Spontaneous mitotic CO rates were measured between *st* and *Sb*. (D–F) Comparison of sensitivities of *Fancm*. Plots show the survival of the indicated phenotype relative to wild-type control flies in the same vial after exposure to (D) 0.002% HN2 (0.1 M), (E) 0.05% MMS (3.23 mM), or (F) IR (1500 rad). Red ●, null; Orange ●, FL; yellow ●, FLKM; green ●, tr; light blue ●, trKM; dark blue ●, wild type (WT). Each dot represents one vial, *n* measures number of vials. Mean percentage of progeny is represented by black horizontal bar. 95% C.I.s are represented by colored error bars. Statistical comparisons were done for *Fancm* compared to each other genotype. Statistically significant comparisons are indicated above error bars; **** $P < 0.0001$ by Kruskal–Wallace test, corrected for multiple comparisons.

of trKM flies reflects functional capacity of the truncated, helicase-dead *Fancm* protein.

The difference in rescue among the transgenes in response to damage by HN2 and IR compared to MMS may represent different functional roles of *Fancm* in various DNA-damage response pathways. The ability of both the FLKM and tr transgene to rescue the sensitivity to HN2 and IR (Figure 4, D and F) is reminiscent of the role of these transgenes in CO prevention (Figure 4C), and again hints at separable functions of *Fancm*: one that is dependent on the helicase and one that is dependent on the C-terminal. Taken together, we propose that *Fancm* regulates or participates in multiple DNA-damage responses.

The ability to rescue sensitivity to MMS (and HN2), is representative of *Fancm* having more than one role in repair. The difference in response to HN2 and MMS in the FLKM and tr may be a result of whether *Fancm* is functioning with other proteins or independently. Kuo *et al.* (2014) investigated functions of *Fancm* that are independent of the FA pathway by comparing phenotypes of *Fancm* mutants to those of *FancI* mutants. Differences in sensitivity suggested a role for *Fancm* in DSB repair that is independent of the FA response.

We hypothesize that *Fancm* not only acts separately from the FA repair response, but can act both catalytically and noncatalytically in repair of DSBs. A catalytic role in the formation of NCO

products might be to unwind short D-loops or to initiate D-loop unwinding. A noncatalytic function might be to recruit HR repair proteins that direct repair toward NCO products, perhaps by extending unwinding of longer D-loops. These dual roles are seen in the FLKM and the tr genotypes. The lack of helicase activity in FLKM prevents it from unwinding D-loops, resulting in some COs being made after these progress to dHJ intermediates. The COs we see in the tr genotype could result from the lack of *Fancm* recruiting HR repair proteins, such as Blm. *Fancm*'s proposed interaction with Blm and involvement with HR and D-loop displacement is supported by studies in humans and yeast (Prakash *et al.* 2005; Nandi and Whitby 2012; Mitchel *et al.* 2013; Kuo *et al.* 2014). *Blm* mutants have more spontaneous mitotic COs than *Fancm* mutants (McVey *et al.* 2007; Kuo *et al.* 2014). Interestingly, *Blm Fancm* double mutants have the same number of mitotic COs as *Fancm* single mutants, consistent with the hypothesis that *Fancm* recruits Blm to prevent COs.

FANCM and its orthologs have been shown to dissociate D-loops, leading to the suggestion that they promote SDSA (Gari *et al.* 2008; Sun *et al.* 2008; Prakash *et al.* 2009). As shown above, *Drosophila Fancm* is also capable of unwinding D-loop-like structures. Use of a gap-repair assay directly demonstrated roles for both *Fancm* and Blm in SDSA in *Drosophila* (Adams *et al.* 2003; Kuo *et al.* 2014). Based on the data

presented above, we propose that one role of Fancm might be to unwind short D-loops, leaving Blm to unwind D-loops that have been extended by additional synthesis or to continue unwinding those initiated by Fancm. In either case, it is possible that Fancm recruits Blm to D-loops. Unfortunately, Kuo *et al.* (2014) were unable to conduct this assay in *Blm Fancm* double mutants and genetic complications prevented us from using our *Fancm* transgenes in the SDSA assay, so these hypotheses cannot be tested with available reagents.

While there are many similarities found between the orthologs of FANCM, there are also many differences that are informative. Some of these can be explained by the assay conditions, but they may also reveal functional divergence. The inability to detect conserved binding motifs is likely a consequence of coevolution between FANCM and other proteins. Regardless, it is clear through this study, as well as work done in other organisms, that FANCM has a broad and diverse role in DNA maintenance and repair.

Acknowledgments

We thank Danielle Rognstad for assistance with the fluorescence anisotropy and Dorothy Erie and members of the Sekelsky laboratory for helpful discussions. This work was supported by grants from the National Institutes of General Medical Sciences to J.S. under award numbers 5RO1 GM-099890 and 1R35 GM-118127. N.-E.R. was supported by grants from the National Institutes of Health Initiative for Maximizing Student Diversity (5R25 GM-055336), a National Science Foundation Graduate Research Fellowship (DGE-1144081), and The Royster Society of Fellows of The Graduate School at the University of North Carolina at Chapel Hill.

Literature Cited

Adams, M. D., M. McVey, and J. Sekelsky, 2003 *Drosophila* BLM in double-strand break repair by synthesis-dependent strand annealing. *Science* 299: 265–267.

Andersen, S. L., and J. Sekelsky, 2010 Meiotic vs. mitotic recombination: two different routes for double-strand break repair: the different functions of meiotic vs. mitotic DSB repair are reflected in different pathway usage and different outcomes. *BioEssays* 32: 1058–1066.

Bassett, A. R., C. Tibbit, C. P. Ponting, and J. L. Liu, 2013 Highly efficient targeted mutagenesis of *Drosophila* with the CRISPR/Cas9 system. *Cell Reports* 4: 220–228.

Brosh, Jr., R. M., 2013 DNA helicases involved in DNA repair and their roles in cancer. *Nat. Rev. Cancer* 13: 542–558.

Ciccio, A., C. Ling, R. Coulthard, Z. Yan, Y. Xue *et al.*, 2007 Identification of FAAP24, a Fanconi anemia core complex protein that interacts with FANCM. *Mol. Cell* 25: 331–343.

Ciccio, A., N. McDonald, and S. C. West, 2008 Structural and functional relationships of the XPF/MUS81 family of proteins. *Annu. Rev. Biochem.* 77: 259–287.

Clauson, C., O. D. Scharer, and L. Niedernhofer, 2013 Advances in understanding the complex mechanisms of DNA interstrand cross-link repair. *Cold Spring Harb. Perspect. Biol.* 5: a012732.

Daley, J. M., H. Niu, and P. Sung, 2013 Roles of DNA helicases in the mediation and regulation of homologous recombination. *Adv. Exp. Med. Biol.* 767: 185–202.

Deans, A. J., and S. C. West, 2009 FANCM connects the genome instability disorders Bloom's Syndrome and Fanconi Anemia. *Mol. Cell* 36: 943–953.

Fujimoto, S., M. Tomschik, and J. Zlatanova, 2009 Does BLM helicase unwind nucleosomal DNA? *Biochem. Cell Biol.* 87: 875–882.

Gari, K., C. Décaillot, A. Z. Stasiak, A. Stasiak, and A. Constantinou, 2008 The Fanconi anemia protein FANCM can promote branch migration of Holliday junctions and replication forks. *Mol. Cell* 29: 141–148.

Gratz, S. J., A. M. Cummings, J. N. Nguyen, D. C. Hamm, L. K. Donohue *et al.*, 2013 Genome engineering of *Drosophila* with the CRISPR RNA-guided Cas9 nuclease. *Genetics* 194: 1029–1035.

Heyer, W. D., K. T. Ehmsen, and J. Liu, 2010 Regulation of homologous recombination in eukaryotes. *Annu. Rev. Genet.* 44: 113–139.

Hoadley, K. A., Y. Xue, C. Ling, M. Takata, W. Wang *et al.*, 2012 Defining the molecular interface that connects the Fanconi anemia protein FANCM to the Bloom syndrome dissolvase. *Proc. Natl. Acad. Sci. USA* 109: 4437–4442.

Huang, M., J. M. Kim, B. Shiotani, K. Yang, L. Zou *et al.*, 2010 The FANCM/FAAP24 complex is required for the DNA interstrand crosslink-induced checkpoint response. *Mol. Cell* 39: 259–268.

Kang, Y. H., P. R. Munashingha, C. H. Lee, T. A. Nguyen, and Y. S. Seo, 2012 Biochemical studies of the *Saccharomyces cerevisiae* Mph1 helicase on junction-containing DNA structures. *Nucleic Acids Res.* 40: 2089–2106.

Khan, I., J. A. Sommers, and R. M. Brosh, Jr., 2015 Close encounters for the first time: Helicase interactions with DNA damage. *DNA Repair (Amst.)* 33: 43–59.

Komori, K., R. Fujikane, H. Shinagawa, and Y. Ishino, 2002 Novel endonuclease in Archaea cleaving DNA with various branched structure. *Genes Genet. Syst.* 77: 227–241.

Komori, K., M. Hidaka, T. Horiuchi, R. Fujikane, H. Shinagawa *et al.*, 2004 Cooperation of the N-terminal Helicase and C-terminal endonuclease activities of Archaeal Hef protein in processing stalled replication forks. *J. Biol. Chem.* 279: 53175–53185.

Koonin, E. V., 1993 A common set of conserved motifs in a vast variety of putative nucleic acid-dependent ATPases including MCM proteins involved in the initiation of eukaryotic DNA replication. *Nucleic Acids Res.* 21: 2541–2547.

Kuo, H. K., S. McMahan, C. M. Rota, K. P. Kohl, and J. Sekelsky, 2014 *Drosophila* FANCM helicase prevents spontaneous mitotic crossovers generated by the MUS81 and SLX1 nucleases. *Genetics* 198: 935–945.

Lafave, M. C., S. L. Andersen, E. P. Stoffregen, J. K. Holsclaw, K. P. Kohl *et al.*, 2014 Sources and structures of mitotic crossovers that arise when BLM helicase is absent in *Drosophila*. *Genetics* 196: 107–118.

Lorenz, A., and M. C. Whitby, 2006 Crossover promotion and prevention. *Biochem. Soc. Trans.* 34: 537–541.

Lorenz, A., F. Osman, W. Sun, S. Nandi, R. Steinacher *et al.*, 2012 The fission yeast FANCM ortholog directs non-crossover recombination during meiosis. *Science* 336: 1585–1588.

Mazón, G., and L. S. Symington, 2013 Mph1 and Mus81-Mms4 prevent aberrant processing of mitotic recombination intermediates. *Mol. Cell* 52: 63–74.

McVey, M., S. L. Andersen, Y. Broze, and J. Sekelsky, 2007 Multiple functions of *Drosophila* BLM helicase in maintenance of genome stability. *Genetics* 176: 1979–1992.

Meetei, A. R., A. L. Medhurst, C. Ling, Y. Xue, T. R. Singh *et al.*, 2005 A human ortholog of archaeal DNA repair protein Hef is

- defective in Fanconi anemia complementation group M. *Nat. Genet.* 37: 958–963.
- Mitchel, K., K. Lehner, and S. Jinks-Robertson, 2013 Heteroduplex DNA position defines the roles of the Sgs1, Srs2, and Mph1 helicases in promoting distinct recombination outcomes. *PLoS Genet.* 9: e1003340.
- Muniandy, P. A., J. Liu, A. Majumdar, S. T. Liu, and M. M. Seidman, 2010 DNA interstrand crosslink repair in mammalian cells: step by step. *Crit. Rev. Biochem. Mol. Biol.* 45: 23–49.
- Nandi, S., and M. C. Whitby, 2012 The ATPase activity of Fml1 is essential for its roles in homologous recombination and DNA repair. *Nucleic Acids Res.* 40: 9584–9595.
- Nishino, T., K. Komori, D. Tsuchiya, Y. Ishino, and K. Morikawa, 2005 Crystal structure and functional implications of *Pyrococcus furiosus* hef helicase domain involved in branched DNA processing. *Structure* 13: 143–153.
- Prakash, R., L. Krejci, S. Van Komen, K. Anke Schurer, W. Kramer *et al.*, 2005 *Saccharomyces cerevisiae* MPH1 gene, required for homologous recombination-mediated mutation avoidance, encodes a 3' to 5' DNA helicase. *J. Biol. Chem.* 280: 7854–7860.
- Prakash, R., D. Satory, E. Dray, A. Papusha, J. Scheller *et al.*, 2009 Yeast Mph1 helicase dissociates Rad51-made D-loops: implications for crossover control in mitotic recombination. *Genes Dev.* 23: 67–79.
- Scheller, J., A. Schurer, C. Rudolph, S. Hettwer, and W. Kramer, 2000 MPH1, a yeast gene encoding a DEAH protein, plays a role in protection of the genome from spontaneous and chemically induced damage. *Genetics* 155: 1069–1081.
- Studier, F. W., 2005 Protein production by auto-induction in high density shaking cultures. *Protein Expr. Purif.* 41: 207–234.
- Studier, F. W., 2014 Stable expression clones and auto-induction for protein production in *E. coli*. *Methods Mol. Biol.* 1091: 17–32.
- Sun, W., S. Nandi, F. Osman, J. S. Ahn, J. Jakovleska *et al.*, 2008 The FANCM ortholog Fml1 promotes recombination at stalled replication forks and limits crossing over during DNA double-strand break repair. *Mol. Cell* 32: 118–128.
- Vinciguerra, P., and A. D. D'andrea, 2009 FANCM: A landing pad for the Fanconi Anemia and Bloom's Syndrome complexes. *Mol. Cell* 36: 916–917.
- Walker, J. E., M. Saraste, M. J. Runswick, and N. J. Gay, 1982 Distantly related sequences in the alpha- and beta-subunits of ATP synthase, myosin, kinases and other ATP-requiring enzymes and a common nucleotide binding fold. *EMBO J.* 1: 945–951.
- Wang, Y., J. W. Leung, Y. Jiang, M. G. Lowery, H. Do *et al.*, 2013 FANCM and FAAP24 maintain genome stability via cooperative as well as unique functions. *Mol. Cell* 49: 997–1009.
- Yang, H., T. Zhang, Y. Tao, F. Wang, L. Tong *et al.*, 2013 Structural insights into the functions of the FANCM-FAAP24 complex in DNA repair. *Nucleic Acids Res.* 41: 10573–10583.
- Yıldız, Ö., H. Kearney, B. C. Kramer, and J. J. Sekelsky, 2004 Mutational analysis of the *Drosophila* DNA repair and recombination gene *mei-9*. *Genetics* 167: 263–273.
- Zheng, X. F., R. Prakash, D. Saro, S. Longrich, H. Niu *et al.*, 2011 Processing of DNA structures via DNA unwinding and branch migration by the *S. cerevisiae* Mph1 protein. *DNA Repair (Amst.)* 10: 1034–1043.

Communicating editor: S. K. Sharan

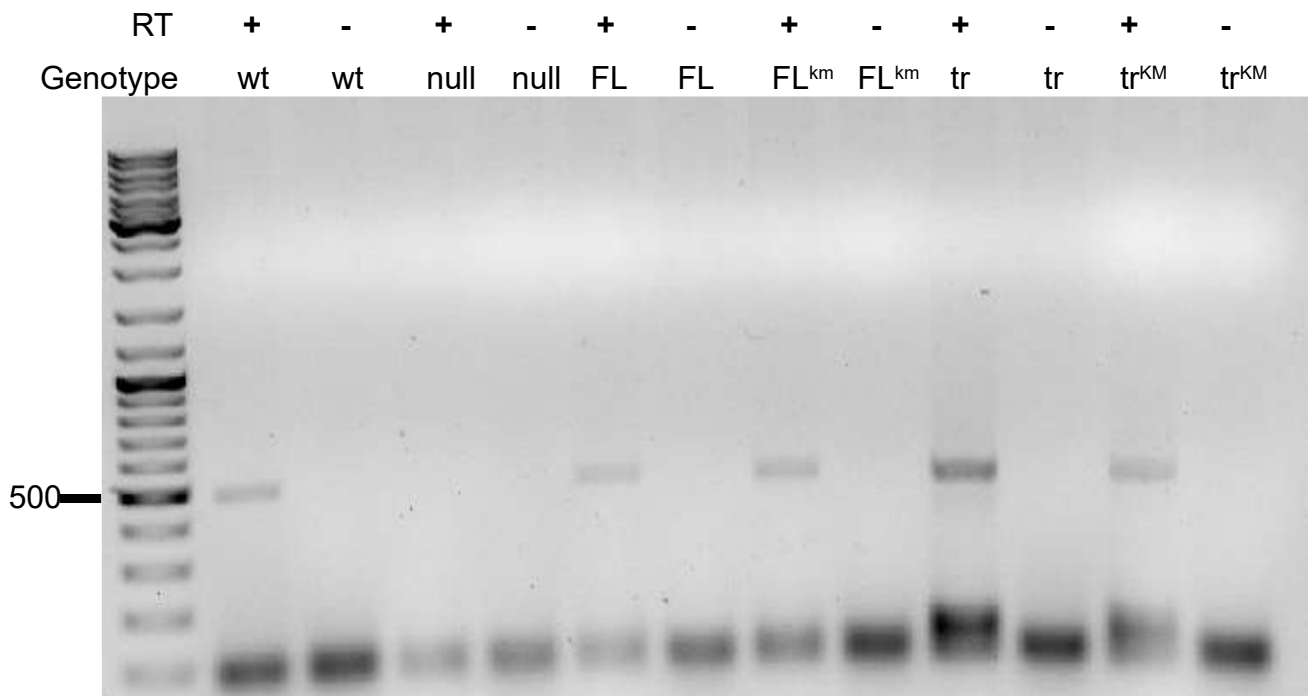


Figure S1- RT reaction for *Fancm* transgenic flies- RT PCR was performed as described in material and methods from whole fly genomic preps. RT was either added (+) or omitted (-), to determine if the presence of a band was the result of genomic contamination. Genotypes represented here are Wildtype (wt) from *yw*¹¹¹⁸; *Fancm*⁰⁶⁹³/*Fancm*^{del} (null); *Fancm*⁰⁶⁹³/*Fancm*^{del} *Sb w*⁺*Fancm*^{FL} (FL); *Fancm*⁰⁶⁹³/*Fancm*^{del} *Sb w*⁺*Fancm*^{FLKM}; *Fancm*⁰⁶⁹³/*Fancm*^{del} *Sb w*⁺*Fancm*^{tr} (tr); *Fancm*⁰⁶⁹³/*Fancm*^{del} *Sb w*⁺*Fancm*^{trKM} (tr^{KM});

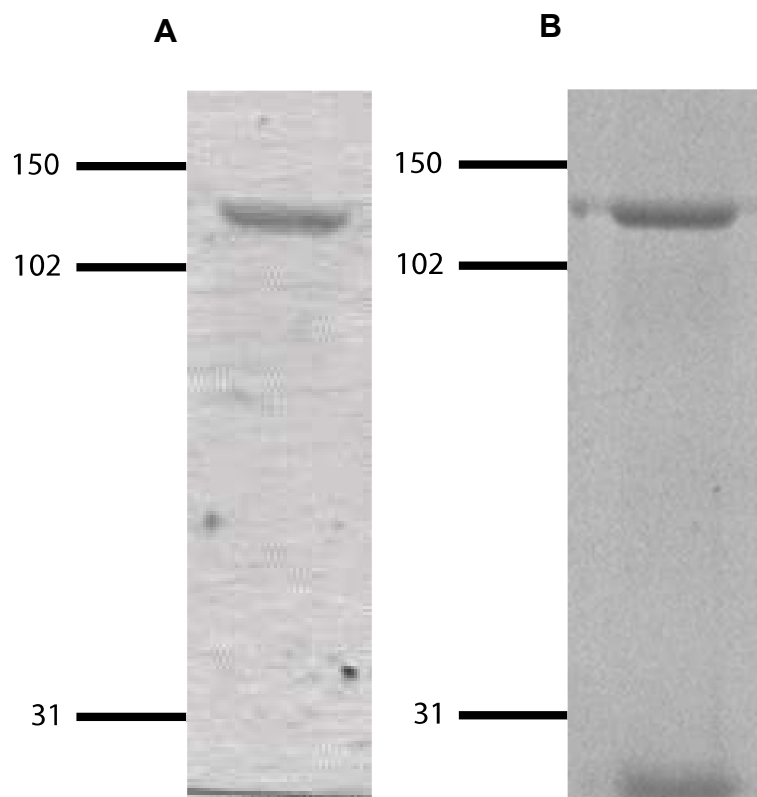
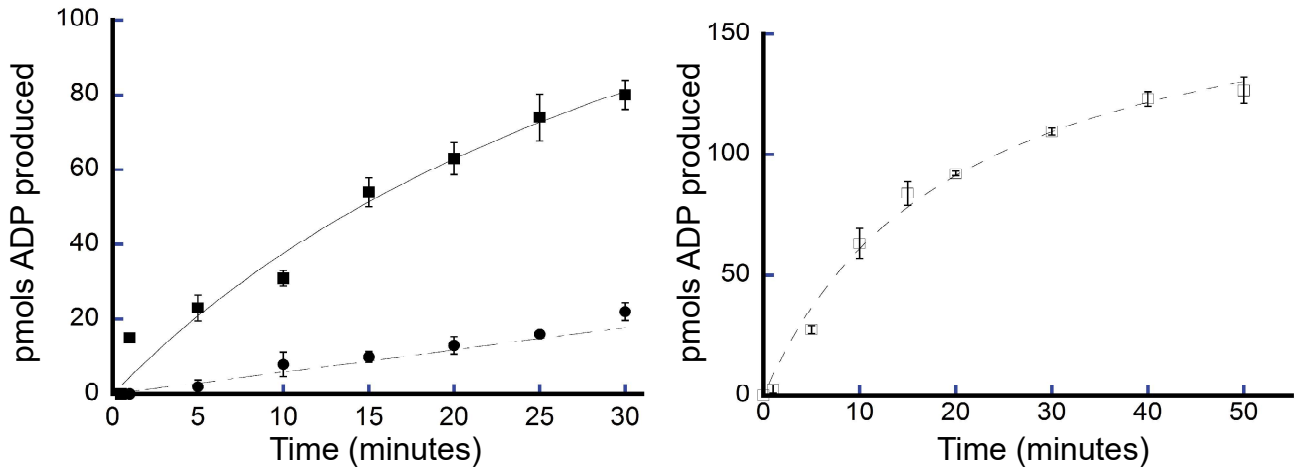


Figure S2- Purification of Fancm Δ and Fancm Δ^{KM} - Fancm Δ and Fancm Δ^{KM} were purified as described in "Materials and Methods". A.) Fancm Δ ; B.) Fancm Δ^{KM} . 100 ng were loaded for each protein.

A ATP hydrolysis as a function of temperature **B** ATP hydrolysis as a function of time



C ATP hydrolysis as a function of [NaCl]

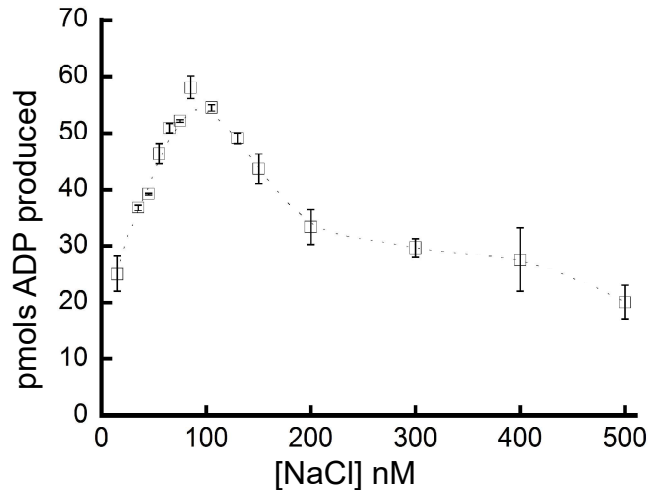


Figure S3- ATP hydrolysis by Fancm. A.) ATP hydrolysis by Fancm as a function of temperature. Fancm ATPase activity was examined as a function of temperature using 212 nM Fancm Δ and M13mp18 ssDNA as the DNA co-factor. All reactions were incubated at 37° (■) or 25° (●) for the time indicated. B.) ATP hydrolysis by Fancm as a function of time. Fancm ATPase activity was examined as a function of time using 212 nM Fancm Δ and M13mp18 ssDNA as the DNA co-factor. All reactions were incubated at 37° for the time indicated. C.) ATP hydrolysis by Fancm as a function of NaCl concentration (nM). Fancm ATPase activity was examined as a function of salt concentration using 212 nM Fancm Δ and M13mp18 ssDNA as the DNA co-factor. All reactions were incubated at 37° for 5 mins. The average values from at least three independent experiments were plotted. Error bars represent standard error about the mean.

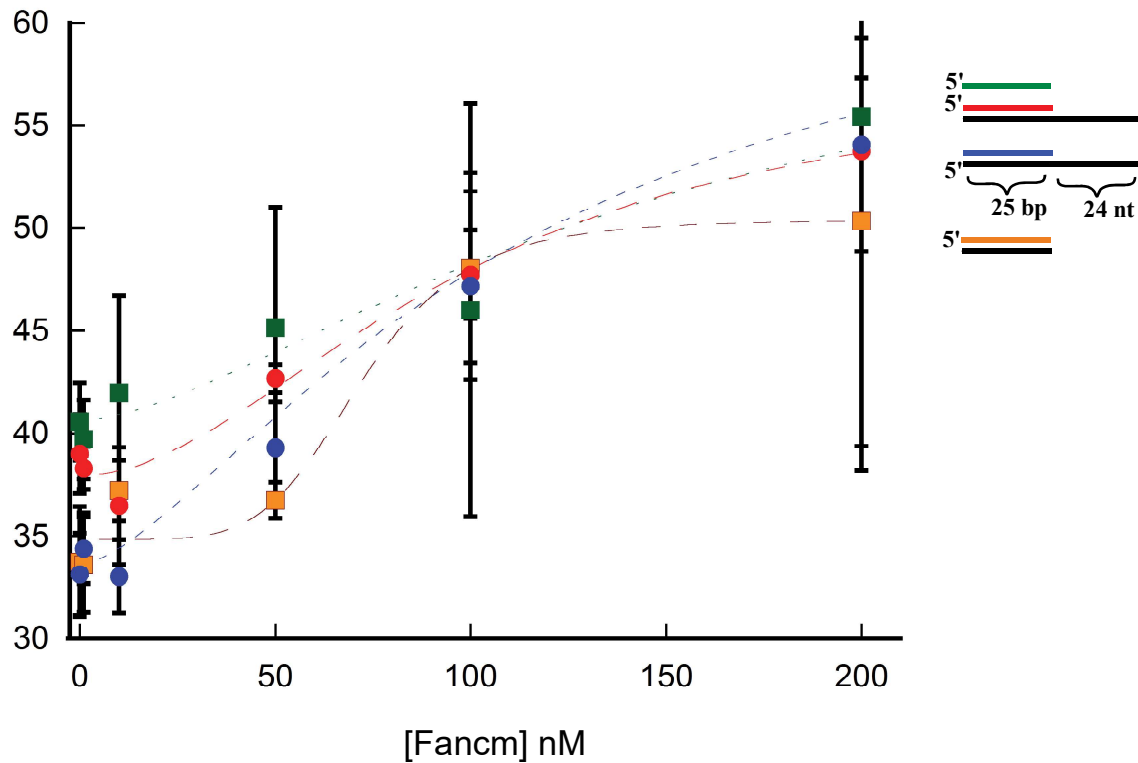


Figure S4- *Fancm* binding of DNA substrates as measured by fluorescence anisotropy. Binding reactions were performed as described under “Materials and Methods”. The indicated concentrations of *Fancm* were incubated with 10 nM of the indicated substrate. Colored strand on each substrate represents the 5' fluorescent strand. Quantitative data from at least 3 experiments were plotted as the average for each protein concentration. Error bars represent the standard deviation about the mean. Oligonucleotides used to make these substrates can be found in Supporting material Table S1. Comparison of substrate bound between *Fancm* Δ on dsDNA (■) (56F/DS), ssDNA (■)(56F); 25 bp duplex region with a 24 nt 5' overhang (●)(56F/5OH); 25 bp duplex region with a 3' 24 nt 3' overhang (●) (56F/3OH).

	1	2	3	4	5	6	7	8	9	10	11
S	0	Δ	Δ^{KM}	MBP	0	Δ	0	Δ	0	Δ	
ATP	+	+	+	+	+	-	-	+	+	-	-
AMP-PNP	-	-	-	-	-	+	+	-	-	-	-
MgCl ₂	+	+	+	+	+	+	+	-	-	+	+

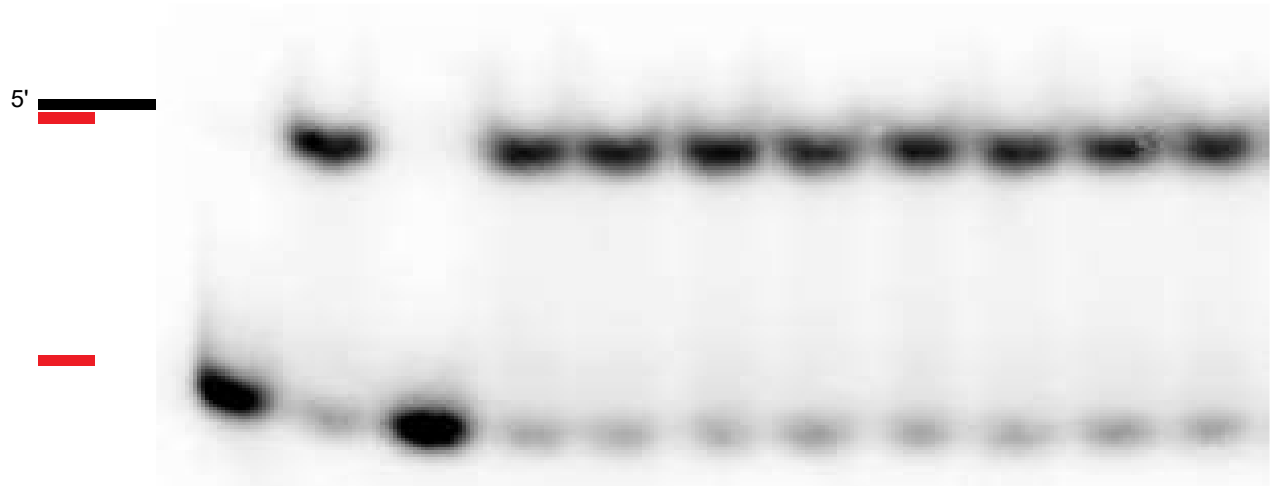


Figure S5- Fancm unwinds duplex DNA in an ATP dependent manner. Protein (212 nM) was incubated with a 5' radiolabeled 15 bp partial duplex with a 25 nucleotide 3' overhang (15/40). Lane 1 is a boiled loading control indicating ssDNA (S); Lanes 2, 6, 8, and 10 are no protein controls (0); Lanes 3, 7, 9, and 11, are Fancm Δ (Δ); Lane 4 is Fancm Δ KM (Δ KM); Lane 5, maltose binding protein (MBP) was used as a negative control. Reactions were performed at 37° for 15 minutes in the presence (+) or absence (-) of ATP, AMP-PNP, and MgCl₂. Colored strand represents radiolabeled strand. Substrate oligonucleotides can be found in Supporting Table S1.

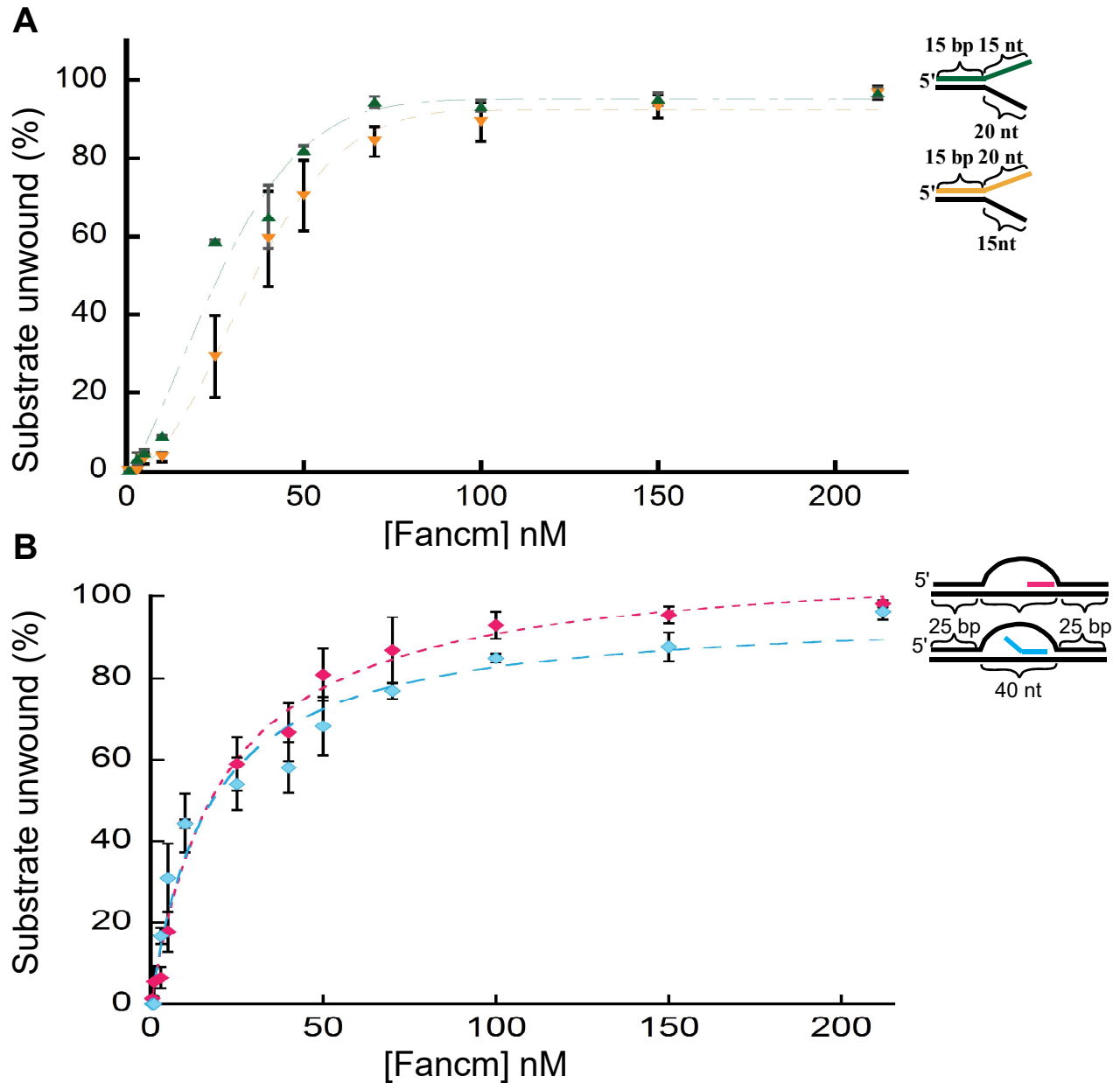


Figure S6- Unwinding of DNA substrates by Fancm. Helicase reactions were performed as described under “Materials and Methods”. The indicated concentrations of Fancm were incubated with 0.1 nM of the indicated substrate. Colored strand on each substrate represents radiolabeled 5’ strand. Quantitative data from at least 3 experiments were plotted as the average for each protein concentration. Error bars represent the standard error about the mean. Oligonucleotides used to make these substrates can be found in Supporting Table S1. A.) Unwinding of splayed arms by Fancm ▼ 15 bp duplex region with 25 nt single stranded 3’ arm and a 15 nt single stranded 5’ arm (SAL/40); ▲ 15 bp duplex region with 15 nt single stranded 3’ arm and a 20 nt single stranded 5’ arm (SAS/40). B.) Unwinding of D-loop intermediate substrates by Fancm. Bubble structures were made using a two 90 nt oligonucleotides with 25 bp of complementary ends with a 40 nt non-complementary middle. ◆ End; ◆ End with a 15 nt 5’ -ssDNA tail.

Table S1: List of oligonucleotides used in this study. (.csv, 2 KB)

Available for download as a .csv file at:

<http://www.genetics.org/lookup/suppl/doi:10.1534/genetics.116.192534/-/DC1/FileS2.xls>